Diamond & Related Materials 18 (2009) 524–527

Contents lists available at ScienceDirect

Diamond & Related Materials

journal homepage: www.elsevier.com/locate/diamond

Dye-sensitized solar cells based on TiO_2–MWCNTs composite electrodes: Performance improvement and their mechanisms

Thanyarat Sawatsuk [a], Anon Chindaduang [a], Chaiyuth Sae-kung [b], Sirapat Pratontep [c], Gamolwan Tumcharern [a,*]

[a] National Nanotechnology Center (NANOTEC), NSTDA, 111 Thailand Science Park, Paholyothin Rd, Klong 1, Klong Luang, Pathumthani 12120 Thailand
[b] Institute of Solar Energy Technology Development (ISET), 111 Thailand Science Park, Paholyothin Rd, Klong 1, Klong Luang, Pathumthani 12120 Thailand
[c] Thai Microelectronics Center (TMEC), NECTEC, NSTDA, 51/4 Moo 1, Wang Takien District, Chachoengsao 24000 Thailand

ARTICLE INFO

Available online 7 November 2008

Keywords:
Carbon nanotubes
Titanium dioxide
Dye-sensitized solar cell

ABSTRACT

We demonstrate that the incorporation of multi-walled carbon nanotubes (MWCNTs) into a TiO_2 active layer contributes to a significant improvement in the energy conversion efficiency of dye-sensitized solar cells (DSSCs). The TiO_2–MWCNTs composite electrode has been prepared by a direct mixing method. The presence of both TiO_2 (anatase) and MWCNTs has been confirmed by Raman spectroscopy, Raman microscopy and Field-Emission Scanning Electron Microscopy (FE-SEM). The performance of DSSCs using the TiO_2–MWCNT composite electrodes is dependent on the MWCNT loading in the electrodes. At optimal conditions, the incorporation of 0.025 wt.% MWCNTs into the conventional working electrode boosts the efficiency by a factor of up to 1.6. The role of MWCNTs in DSSCs has been investigated by the electrochemical impedance spectroscopy. The improvement in energy conversion efficiency is correlated not only with increased photocurrent and electrical double layer capacitance, but also with a decrease in the electrolyte|electrode interfacial resistance and the Warburg impedance. At high MWCNT loading, the conductivity of the electrodes decreases, which may result from the MWCNT agglomeration and the loss of optical transparency.

1. Introduction

Carbon nanotubes (CNTs) are considered remarkable materials owing to their unique structural and mechanical properties such as high electrochemical stability, low resistivity, and high surface-to-volume ratio [1–3]. In general, carbon nanotubes can be divided into two categories: single-wall carbon nanotubes (SWCNTs) and multi-wall carbon nanotubes (MWCNTs). Depending on the folding angle and the diameter, SWCNTs may be metallic, insulating or semiconducting [4], whereas MWCNTs are all conductive. Applications of carbon nanotubes include molecular sensors [5], organic field-effect transistors (OFET) [6] and dye-sensitized solar cells (DSSCs) [7].

Dye-Sensitized Solar Cells (DSSCs) or Grätzel solar cells were first invented by Michael Grätzel in 1991 [2]. Owing to their low fabrication cost and high energy conversion performance [8,9], DSSCs are a promising future generation of solar energy devices. DSSCs comprise two electrochemical electrodes with an iodide-based electrolyte. Despite the initial success of an 11.1% solar conversion efficiency [2], efforts to further improve their performance have yielded little progress. A major hurdle in attaining higher energy conversion efficiency is the transport of electrons across the nanometer-sized particle network inside the electrodes. Recent studies on the efficiency improvements have been focused on incorporating carbon nanotubes into the working electrodes [10–12] or improving ionic liquid electrolytes [13]. The working or front DSSC electrode is generally composed of active titanium dioxide (TiO_2) semiconductors and dye molecules [2]. Concerning DSSCs and carbon nanotubes, the more common approach utilizes well-align carbon nanotubes fabricated by high cost vacuum-based techniques such as reactive sputtering or chemical vapour deposition (CVD) [3]. Recently, an enhancement of the DSSC energy conversion efficiency by a factor of two has been achieved by using TiO_2-decorated SWCNT films [14].

In this report, using a simple direct mixing method, we describe preparation and characterization of a TiO_2–MWCNT composite used as the materials for the DSSC working electrode. The energy conversion efficiency and the electrochemical impedance of the fabricated cells have been determined. With this method, no orderly arrangements of CNTs have been observed on the conductive substrate; however, a comparable improvement in the energy conversion efficiency of our DSSCs to those with well aligned CNT electrodes has been achieved. Importantly, our technique is compatible to a large scale production using existing DSSC fabrication technology.

2. Experiments

MWCNTs with a mean diameter of 20 nm were provided by Bayers Materials (Thailand and Germany). The TiO_2–MWCNT composites were prepared by dispersing TiO_2 nanopowder (anatase, 100 mg),

* Corresponding author. Tel.: +662 564 7100x6587; fax: +662 564 6989.
E-mail address: gamolwan@nanotec.or.th (G. Tumcharern).

0925-9635/$ – see front matter
doi:10.1016/j.diamond.2008.10.052

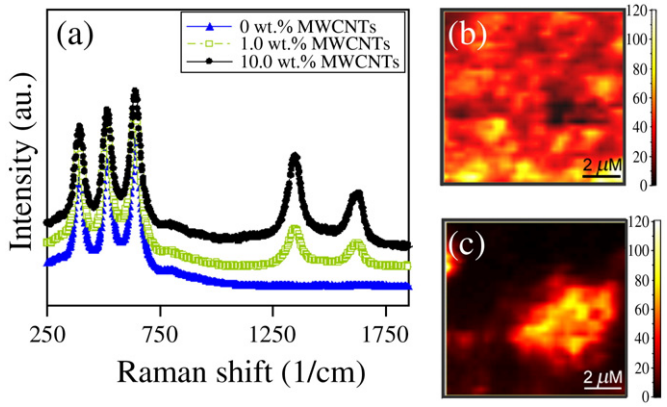

Fig. 1. Raman spectroscopy and mapping of TiO_2–MWCNT composite films: (a) Raman spectra of TiO_2 and TiO_2–MWCNT films and (b, c) confocal Raman mapping images of TiO_2–MWCNT (10%wt) films using the 642 cm^{-1} TiO_2 Raman peak and 1348 cm^{-1} D line of MWCNTs.

MWCNT (0–10%wt) and ethyl cellulose (100 mg) in terpineol using ultrasonication. TiO_2–MWCNT films on ITO glass substrates (2×3 cm, a sheet resistance of 10 Ω per square, Bangkok Solar cell Ltd.) were fabricated by screen-printing with an active area of 0.36 cm^2 and were annealed at 500 °C.

Raman spectra of the TiO_2–MWCNT films were taken by the NTMDT Ntegra spectra AFM confocal Raman system with the 632.8 nm excitation. The images were recorded using a 60x objective. Field-Emission Scanning Electron Microscope (FE-SEM, Hitachi S-4700) images and optical absorption spectra (Perkin Elmer Lambda 650) were obtained from the TiO_2–MWCNT films with an active area of 1 cm^2. Electrochemical properties were investigated by using the Eco Chemie Autolab PGSTAT302 with the General-Purpose Electrochemical System (GPES) software and the Frequency Response Analyzer (FRA2) module. A conventional cell with a three-electrode configuration was used throughout our electrochemical characterization: the TiO_2–MWCNTs films on conductive glass substrates as a working electrode, a platinum auxiliary electrode and a Ag/AgCl reference electrode. The electrolyte was an aqueous solution of 0.1 mM $K_3Fe(CN)_6$ in 1 M KCl.

For the DSSC fabrication, the annealed $TiOs_2$–MWCNT films were soaked in an ethanol solution of Ru(II)L_2(NCS):2TBA (L=2,2′-bipyridyl-4,4′-dicarboxylate, TBA=tetrabutyl ammonium). The TiO_2–MWCNT composite electrodes and the conventional Pt electrodes were assembled face-to-face, then filled with an acetonitrile electrolyte solution containing LiI, I_2, and 1-methyl-3-propylimidazolium iodide.

The solar power conversion efficiency of DSSCs was measured from the photocurrent-voltage characteristics with a transient photocurrent under the AM 1.5 irradiation (100 mW·cm^{-2}). In addition, the electrochemical impedance analyses of the complete DSSCs fabricated by the above methods were investigated using the potentiostat/galvanostat. The spectra were recorded over a frequency range of 1 MHz to 0.1 Hz with an ac amplitude of 10 mV under the white light irradiation (1.3 mW·cm^{-2}).

3. Results and discussions

In Fig. 1 (a), the anatase form of TiO_2 represents by three Raman peaks at approximately 395, 518, and 642 cm^{-1} [15]. Other two peaks at approximately 1348 and 1624 cm^{-1} indicate the D and the G lines of MWCNTs, respectively [16]. The absence of the RBM band and the G–G' splitting in the Raman spectra could be explained by the weak signal of a large inner-diameter of the tubes and some distribution of the MWCNT diameter, respectively [17]. The Raman results confirm the presence of MWCNT in the DSSC front electrode after the fabrication processes. In addition, the distribution of MWCNTs in the TiO_2 matrix was investigated by confocal Raman mapping [18], which was conducted only on the composite films with high MWCNT concentration (10%wt). The Raman mapping was obtained by using the 642 cm^{-1} TiO_2 Raman peak (Fig. 1 (b)) and the 1348 cm^{-1} D line of MWCNTs (Fig. 1 (c)). The color bar on the right side of each image indicates the Raman intensity, hence relative material concentration. The Raman mapping results therefore indicate some aggregation (in the micron range) of MWCNTs in the anatase TiO_2.

The surface morphology of the annealed TiO_2 (Fig. 2 (a)) and TiO_2–MWCNT (Fig. 2 (b)) films was further characterized by FE-SEM. Note that some MWCNT aggregation is also observed with the FE-SEM. Nevertheless, both FE-SEM images display a similar surface structure of TiO_2 with coarse grains of approximately 1 μm in size. Therefore, the incorporation of MWCNTs should not significantly alter the surface area of TiO_2.

Fig. 3 illustrates the optical absorption spectra of TiO_2–MWCNT films. Compared to the conventional TiO_2 films, the optical absorption for the film containing 0.1 wt.% MWCNTs remains approximately unchanged. Increased MWCNT loading (≥0.5%wt) resulted in higher optical absorption of the composite film.

Electrochemical characteristics of the TiO_2–MWCNT (0–0.2%wt) composite electrodes were studied by cyclic voltammetry (CV). Fig. 4 (a) shows cyclic voltammograms of TiO_2 films containing 0.1 wt.% MWCNTs, using the scan rate of 10 to 300 mV·s^{-1}. An increase in anodic (i_{pa}) and cathodic (i_{pc}) peak currents can be observed when the scan rate rises (Fig. 4 (b)). A linear correlation of the peak current (i_p) and the square root of the scan rate ($v^{-1/2}$) has been found, which implies that the diffusion process of $Fe(CN)_6^{3-}/Fe(CN)_6^{4-}$ species occurs at the surface of TiO_2–MWCNT electrode. The expansion of ΔE_p observed at higher scan rates suggests that these processes change from reversible to quasi-

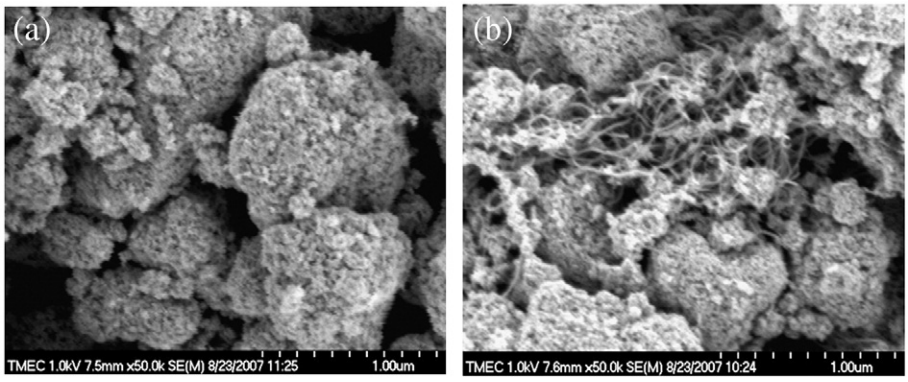

Fig. 2. FE-SEM images of (a) TiO_2 and (b) TiO_2–MWCNT (10%wt) films.

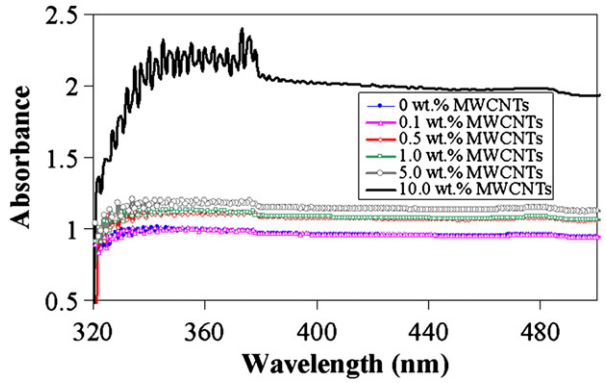

Fig. 3. Optical absorption spectra of TiO_2 and TiO_2–MWCNT films.

reversible. In addition, the plots of i_p against $\nu^{1/2}$ remain linear in the investigated range of MWCNT concentration, suggesting that the incorporated MWCNTs should not substantially affect the electron transfer mechanism at the electrolyte|electrode interface. The correlation of i_p with the MWCNT concentration in the TiO_2 films is displayed in Fig. 4 (c) and (d). The largest increase in i_p is observed between the MWCNT concentration of 0 and 0.025%wt. Then, at higher MWCNT concentrations, the peak current increases gradually and levels out at the MWCNTs loading of >0.075%wt. This saturation may be caused by the MWCNT agglomeration, such as those observed by the Raman mapping and the FE-SEM. The reproducible CVs up to 50 cycles of all electrodes are also observed, indicating that the TiO_2–MWCNT electrodes should be sufficiently stable for the DSSC application.

Table 1
J–V characteristics of TiO_2–MWCNT front electrode of the DSSCs

MWCNTs (%wt)	V_{oc} (V)	J_{sc} (mA/cm^2)	FF	η (%)
0	0.76	14.41	0.58	6.31
0.01	0.78	14.41	0.60	6.77
0.02	0.79	17.25	0.72	9.79
0.025	0.79	16.99	0.77	10.29
0.03	0.78	12.38	0.59	5.67
0.05	0.74	11.81	0.52	4.57
0.075	0.69	11.12	0.49	3.75
0.1	0.68	11.11	0.46	3.52

The *J–V* characteristics of the DSSCs under the AM 1.5 illumination standard with an active area of 0.36 cm^2 are reported in Table 1. The open-circuit voltage (V_{oc}), short-circuit current (J_{sc}), filling factor (*FF*), and efficiency (η) for different MWCNT loadings are in correlation with both electrochemical and optical properties of the composite films. At the best conditions, the incorporation of MWCNTs at 0.025%wt in the TiO_2 films increases the conversion efficiency by approximately 50%, compared to the conventional DSSCs. The strong enhancement of J_{sc} with only a slight increase in V_{oc} of the DSSCs with 0.025 wt.% MWCNTs suggests that MWCNTs should play an important role in enhancing the conductivity of the TiO_2 films. However, at higher MWCNT contents, the solar conversion efficiencies decrease, which should be

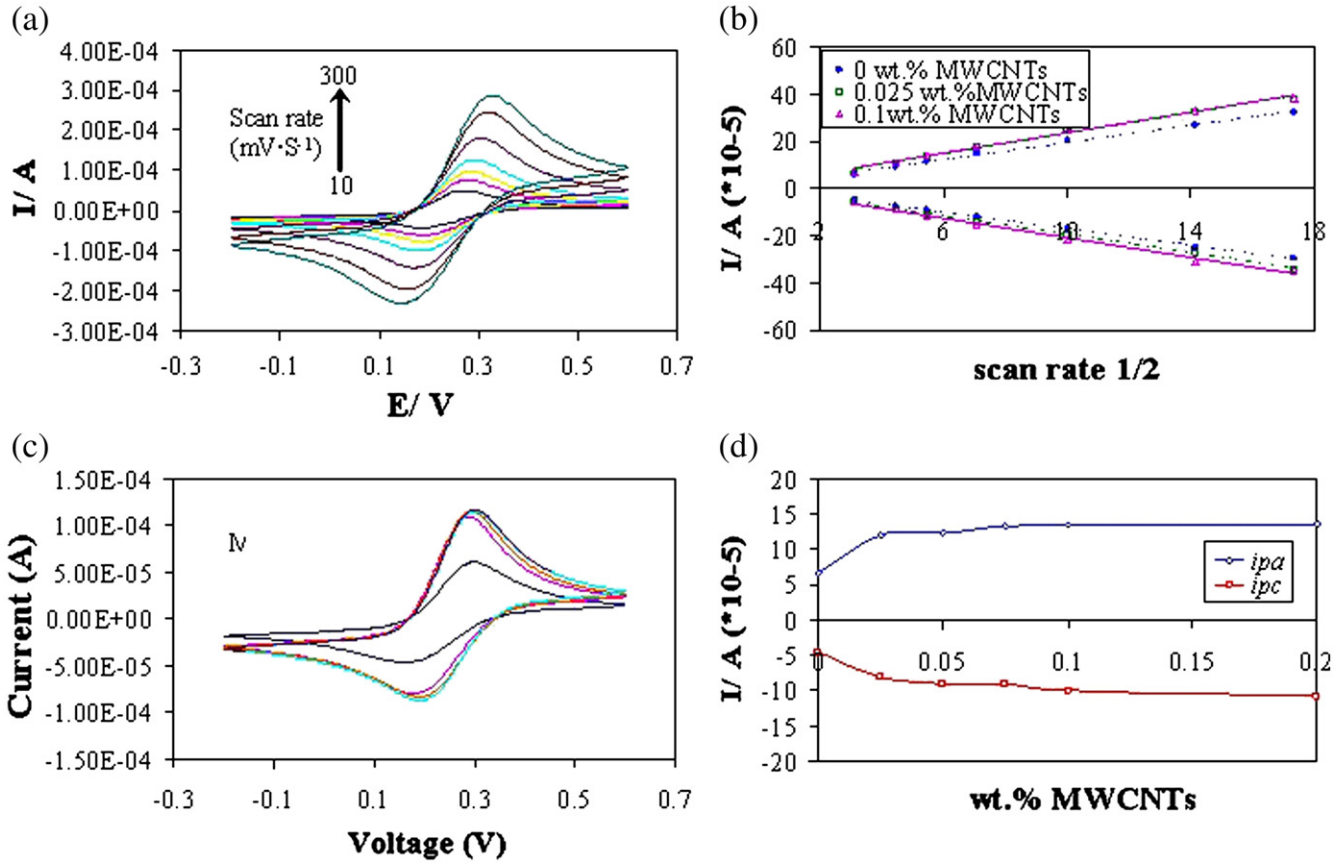

Fig. 4. Electrochemical analysis of the TiO_2–MWCNT composite films: (a) Cyclic voltammograms of $K_3Fe(CN)_6$ using TiO_2–MWCNT (0.1%wt) films as the working electrode at different scan rates (from inside out: 10, 20, 30, 50, 100, 200, and 300 mV·S^{-1}) and (b) the variation of i_p (◊ i_{pa} and □ i_{pc}) as a function of $\nu^{1/2}$ for the TiO_2–MWCNT electrodes (0, 0.025, and 0.1 wt.% MWCNTs) in 0.1 mM $K_3Fe(CN)_6$/1 M KCl at scan rates of 10–300 mV·S^{-1}. The linear regression equations of anodic peaks of 0, 0.025, and 0.1 wt.% MWCNTs are expressed as $y=1.7999x+1.5727$, $y=2.207x+1.3349$ and $y=2.177x+1.9391$, respectively. The linear regression equations of cathodic peaks of 0, 0.025, and 0.1 wt.% MWCNTs are expressed as $y=-1.7643x+0.642$, $y=-1.9718x+0.1809$ and $y=-2.1122x+0.2964$, respectively. (c) Cyclic voltammograms of $K_3Fe(CN)_6$ using TiO_2 films at different MWCNT loadings (from inside out: 0, 0.025, 0.05, 0.075, 0.1 and 0.2%wt) at a scan rate of 100 mV·S^{-1} and (d) the variation of i_p with %wt of MWCNTs in the composite films (◊ i_{pa} and □ i_{pc}).

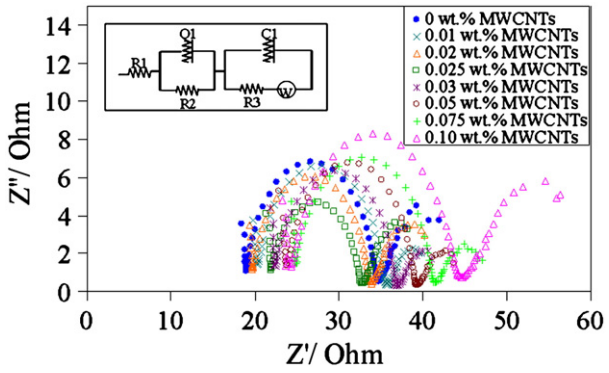

Fig. 5. Nyquist plots of DSSCs with TiO_2–MWCNT electrodes at different MWCNT loadings: (♦) 0, (■) 0.010, (▲) 0.020, (●) 0.025, (◊) 0.030, (○) 0.050, (□) 0.075 and (△) 0.10%wt. Inset: the equivalent circuit model of DSSCs containing TiO_2–MWCNT electrodes.

explained by the solar energy loss from the optical absorption of the carbon materials. This result in a lower initial photocurrent generated by the dye molecules, hence a lower current measured in the external circuit.

The Electrochemical Impedance Spectroscopy (EIS) of the fabricated DSSC cells using the TiO_2–MWCNT composite electrodes has been investigated in order to correlate the device structure with an equivalent circuit model, and to gain understandings of the kinetics of electrochemical and photoelectrochemical processes [19,20]. A typical Nyquist diagram of DSSCs consists of three semi-circles, which represent the redox reaction at the platinum counter electrode (high frequency), the electron transfer at the TiO_2|dye|electrolyte interface (medium frequency), and the carrier transport by ions in the electrolyte (low frequency) [21]. The Nyquist plots of the DSSCs containing 0–0.1%wt of MWCNTs in the front electrodes are shown in Fig. 5. The equivalent circuit model [22] is displayed in the inset of Fig. 5. The ohmic serial resistances in the model circuit are R_1, R_2 and R_3, for the electrolyte| conductive glass, the platinum electrode, and dye|electrolyte|TiO_2–MWCNT interfaces, respectively. Q_1 presents the capacitance at the TiO_2| conductive glass interface. The DSSCs containing 0.025 wt.% MWCNTs, which yielded the highest efficiency, resulted in the smallest semi-circle in the medium frequency range of the electrochemical impedance spectra. This should originate from the highest electrical double layer capacitance at the electrolyte|TiO_2|MWCNT interface (C_1), the lowest resistance at the dye|electrolyte|TiO_2–MWCNT interface (R_3), and the lowest Warburg impedance of the diffusion of the I^-/I_3^- species in the electrolyte (W).

4. Conclusions

The performance of DSSCs with TiO_2–MWCNT composite films as the working electrode has been substantially improved in comparison to the conventional DSSC by using the direct mixing technique. The role of MWCNTs in the solar energy conversion enhancement was investigated principally by the electrochemical impedance analysis of the entire fabricated cells. At low MWCNT concentrations up to 0.025%wt, both the electrical double layer capacity and the conductivity at the electrolyte| TiO_2|MWCNT interface were distinctly improved. At higher MWCNTs concentrations in the composite electrode, however, we found a degradation of the DSSC performance, which may result from an increase in the optical absorbance of the composite electrode and possibly from some MWCNT aggregation. Thus double-layer capacity, electrical conductivity, and optical absorption play a major role in the enhancement of the energy conversion efficiency of the MWCNT-incorporated DSSCs. In addition, the reproducibility of the CV measurements up to 50 cycles ensure that the direct mixing method, which is suitable for large scale production, is capable of producing the electrodes with sufficient stability for the DSSC application.

Acknowledgements

The authors are grateful for the research funding from the Institute of Solar Energy Development, National Science and Technology Development Agency, Thailand (Funding number: B22 AR0101). We also thank Mr. Matthias Hanusch for supplying synthesized imidazole and Bayer Materials (Germany and Thailand) for providing the MWCNTs.

References

[1] M.K. Nazeeruddin, A. Kay, I. Rodicio, R. Humphry-Baker, E. Müller, P. Liska, N. Vlachopoulos, M. Grätzel, J. Am. Chem. Soc. 115 (1993) 6382.
[2] B. O ' Regan, M. Grätzel, Nature 353 (1991) 737.
[3] Y.-J. Park, S.-C. Park, W.-C. Jung, J.-G. Nam, H.-J. Kim, US Patent (Patent Application) US2006/137741 A1.
[4] M. Paradise, T. Goswami, Mater. Des. 28 (2007) 1477.
[5] C. Li, E.T. Thostenson, T.-W. Chou, Compos. Sci. Technol. 68 (2008) 1227.
[6] W. Wu, W. Xu, W. Hu, Y. Liu, D. Zhu, Chem. Bull. (Huaxue Tongbao) 69 (2006) 404.
[7] T.Y. Lee, J.-B. Yoo, Diamond Relat. Mater. 14 (2005) 1888.
[8] M. Grätzel, J. Photochem. Photobiol. C: Photochem. Rev. 4 (2003) 145.
[9] A. Kay, M. Grätzel, Sol. Energy Mater. Sol. Cells 44 (1996) 99.
[10] S.-R. Jang, R. Vittal, K.-J. Kim, Langmuir 20 (2004) 9807.
[11] T.Y. Lee, P.S. Alegaonkar, J.-B. Yoo, Thin Solid Films 515 (2007) 5131.
[12] S.L. Kim, S.-R. Jang, R. Vittal, J. Lee, K.-J. Kim, J. Appl. Electrochem. 36 (2006) 1433.
[13] H. Usui, H. Matsui, N. Tanabe, S. Yanagida, J. Photochem. Photobiol., A Chem. 164 (2004) 97.
[14] A. Kongkanand, R. Martínez Domínguez, P.V. Kamat, Nano Lett. 7 (2007) 676.
[15] P.-T. Hsiao, K.-P. Wang, C.-W. Cheng, H. Teng, J. Photochem. Photobiol., A Chem. 188 (2007) 19.
[16] P. Rai, D.R. Mohapatra, K.S. Hazra, D.S. Misra, J. Ghatak, P.V. Satyam, Chem. Phys. Lett. 455 (2008) 83.
[17] M.S. Dresselhaus, G. Dresselhaus, R. Saito, A. Jorio, Phys. Rep. 409 (2005) 47.
[18] H. Kuzmany, W. Plank, M. Hulman, C. Kramberger, A. Gruneis, T. Pichler, H. Peterlik, H. Kataura, Y. Achiba, Eur. Phys. J. B 22 (2001) 307.
[19] A.J. Bard, L.R. Faulkner, Electrochemical Methods: Fundamentals and Applications, second ed., John Wiley & Sons, New York, 2001, p. 368.
[20] Q. Wand, J.-E. Moser, M. Grätzel, J. Phys. Chem., B 109 (2005) 14945.
[21] N. Koide, A. Islam, Y. Chiba, L. Han, J. Photochem. Photobiol., A Chem. 182 (2006) 296.
[22] K.-M. Lee, V. Suryanarayanan, K.-C. Ho, Sol. Energy Mater. Sol. Cells 91 (2007) 1416.